Accelerated Publications

Monitoring Water Reactions during the S-State Cycle of the Photosynthetic Water-Oxidizing Center: Detection of the DOD Bending Vibrations by Means of Fourier Transform Infrared Spectroscopy[†]

Hiroyuki Suzuki,[‡] Miwa Sugiura,[§] and Takumi Noguchi*[,‡]

Institute of Materials Science, University of Tsukuba, Tsukuba, Ibaraki 305-8573, Japan, and Cell-Free Science and Technology Research Center, Ehime University, Matsuyama, Ehime 790-8577, Japan

Received August 22, 2008; Revised Manuscript Received September 14, 2008

ABSTRACT: Photosynthetic water oxidation takes place in the water-oxidizing center (WOC) of photosystem II (PSII). To clarify the mechanism of water oxidation, detecting water molecules in the WOC and monitoring their reactions at the molecular level are essential. In this study, we have for the first time detected the DOD bending vibrations of functional D_2O molecules during the S-state cycle of the WOC by means of Fourier transform infrared (FTIR) difference spectroscopy. Flash-induced FTIR difference spectra upon S-state transitions were measured using the PSII core complexes from *Thermosynechococcus elongatus* moderately deuterated with $D_2{}^{16}O$ and $D_2{}^{18}O$. $D_2{}^{16}O$-minus-$D_2{}^{18}O$ double difference spectra at individual S-state transitions exhibited six to eight peaks arising from the $D^{16}OD/D^{18}OD$ bending vibrations in the 1250−1150 cm^{-1} region. This observation indicates that at least two water molecules, not in any deprotonated forms, participate in the reaction at each S-state transition throughout the cycle. Most of the peaks exhibited clear counter peaks with opposite signs at different transitions, reflecting a series of reactions of water molecules at the catalytic site. In contrast, negative bands at ∼1240 cm^{-1} in the $S_2 \rightarrow S_3$, $S_3 \rightarrow S_0$, and possibly $S_0 \rightarrow S_1$ transitions, for which no clear counter peaks were found in other transitions, can be interpreted as insertion of substrate water into the WOC from a water cluster in the proteins. The characteristics of the weakly D-bonded OD stretching bands were consistent with the insertion of substrate from internal water molecules in the $S_2 \rightarrow S_3$ and $S_3 \rightarrow S_0$ transitions. The results of this study show that FTIR detection of the DOD bending vibrations is a powerful method for investigating the molecular mechanism of photosynthetic water oxidation as well as other enzymatic reactions involving functional water molecules.

Water functions as a terminal electron donor to reduce CO_2 in oxygenic photosynthesis. The water oxidation takes place at the water-oxidizing center (WOC)[1] in photosystem II (PSII) protein complexes (*1*−*4*). The X-ray crystallographic structures of the PSII core complexes from *Thermosynechococcus elongatus* at 3.0−3.5 Å resolution (*5, 6*) together with the information from EXAFS studies (*7*) revealed that the WOC consists of a Mn_4Ca cluster surrounded by carboxylate and histidine ligands. Because of the limited resolutions of the X-ray structures and possible damage by X-ray radiation (*8, 9*), however, the proposed structural models are still controversial (*5*−*7*). In addition, no information about the locations of water molecules is available in the current X-ray structures.

In the WOC, two water molecules are converted into one molecular oxygen and four protons through a light-driven cycle, the so-called S-state cycle, consisting of five intermediates (S_i states, where $i = 0$−4) (*1*−*4*). Among them, the S_1 state is the most dark stable, and flash illumination advances each S state to the next state ($S_1 \rightarrow S_2 \rightarrow S_3 \rightarrow S_0 \rightarrow S_1$). Molecular oxygen is released during the $S_3 \rightarrow S_0$ transition via the transient S_4 state. The molecular mechanism of water oxidation, however, remains largely unknown.

In attempting to understand the mechanism of water oxidation, spectroscopic detection of substrate and its reaction is of utmost importance. Mass spectrometric measurements have shown that the rate of ^{18}O incorporation has biphasic kinetics throughout the S states, representing two distinct substrate molecules with fast and slow exchange rates (*10, 11*). Several exchangeable protons, including those from substrate water, have been detected in the vicinity of the Mn cluster

[†] This study was supported by Grants-in-Aid for Scientific Research (17GS0314) from the Ministry of Education, Culture, Sports, Science and Technology to T.N. and a Grant-in-Aid for JSPS Fellows (19252) to H.S.

* To whom correspondence should be addressed. Phone: +81-29-853-5126. Fax: +81-29-853-4490. E-mail: tnoguchi@ims.tsukuba.ac.jp.

[‡] University of Tsukuba.

[§] Ehime University.

[1] Abbreviations: FTIR, Fourier transform infrared; Mes, 2-(*N*-morpholino)ethanesulfonic acid; PSII, photosystem II; WOC, water-oxidizing center.

10.1021/bi801580e CCC: $40.75
Published on Web 09/27/2008

in the S_0, S_1, and S_2 states using the ENDOR and ESEEM techniques (*12*−*16*). Also, a water-exchangeable oxygen strongly coupled to the Mn cluster in the S_2 state was recently detected by ^{17}O-HYSCOPE spectroscopy (*17*).

Another powerful method of directly detecting water molecules in the WOC is Fourier transform infrared (FTIR) spectroscopy. Using a light-induced FTIR difference technique, structural changes of the WOC, including the Mn cluster core, amino acid ligands, polypeptide chains, and water molecules, upon S-state transitions have been detected (reviewed in refs *18*−*23*). The reactions of water molecules were detected as the OH and OD stretching vibrations in the regions of 3800−3000 and 2800−2200 cm^{-1}, respectively (*23*−*25*). From the weakly hydrogen-bonded OH(D) bands, which exhibited relatively sharp peaks on the higher-frequency side of the OH(D) region, the symmetry change in the hydrogen bond interaction of an active water in the $S_1 \rightarrow S_2$ transition and proton release reactions and/or shifts from weak to strong hydrogen bonding in the other three transitions have been proposed (*23*−*25*). However, more accurate analyses of water reactions by FTIR spectroscopy have been hampered by the inherent broad features of strongly hydrogen-bonded OH(D) bands.

Another vibration of water is the HOH bending mode, which shows a band at ∼1640 cm^{-1} in liquid water (*26*). The HOH bending band is also sensitive to hydrogen bond interactions (*27, 28*), while it is not significantly broadened by strong hydrogen bonding. In addition, since this vibration disappears upon deprotonation, it is suitable for monitoring water reactions that include proton release steps. Thus, this vibration appears to be a useful marker for analyzing the water reactions in the WOC as well as in other proteins involving functional water in the active sites. Unfortunately, however, the HOH bending band often shows a weak intensity relative to the OH stretching bands (*26*), and in addition, in proteins it heavily overlaps with the amide I bands arising from backbone amides, which usually exhibit strong, complex features in FTIR difference spectra and are sensitive to subtle changes in sample conditions. Hence, attempts to detect the HOH bending vibrations of water molecules in the WOC have not been successful so far.

We report here, for the first time, detection of the DOD bending vibrations of D_2O molecules in flash-induced FTIR difference spectra during the S-state cycle of the WOC. The DOD bending bands appear around 1210 cm^{-1} (*26*), where proteins do not exhibit any strong bands. Several DOD peaks were identified by $D_2{}^{18}O$ substitution in the spectra of the individual S-state transitions, reflecting the reactions of water molecules including substrate at the catalytic site of the WOC.

MATERIALS AND METHODS

The PSII core complexes from the *T. elongatus* 43-H strain, in which the carboxyl terminus of the CP43 subunit was genetically histidine-tagged, were purified using Ni^{2+} affinity column chromatography as described previously (*29*). The complexes were suspended in a 10 mM Mes-NaOH (pH 6.0) buffer containing 5 mM NaCl, 5 mM $CaCl_2$, and 0.06% *n*-dodecyl β-D-maltoside and concentrated to ∼4.5 mg of Chl/mL using a Microcon-100 apparatus (Amicon). An aliquot of the sample suspension (7 μL) was mixed with 2 μL of 100 mM potassium ferricyanide and dried on a BaF_2 plate (25 mm in diameter) under N_2 gas with an oval shape (6 mm × 9 mm). We moderately hydrated (or deuterated) the sample under 95% relative humidity by placing 3 μL of a 40% (v/v) glycerol/water solution in a sealed IR cell without touching the sample (*30*). For hydration, glycerol/$H_2{}^{16}O$ (natural abundance) and glycerol/$H_2{}^{18}O$ (Euriso-top, 95.44 atom % ^{18}O) mixtures were used, and for deuteration, glycerol$(OD)_3$ (CDN, 98.7 atom % D)/$D_2{}^{16}O$ (CDN, 99.9 atom % D) and glycerol$(OD)_3$/$D_2{}^{18}O$ (ICON, 99 atom % D, 95 atom % ^{18}O) mixtures were used. The sample temperature was kept at 10 °C by circulating cold water in a copper holder.

Flash-induced FTIR difference spectra during the S-state cycle were recorded using a Bruker IFS-66/S spectrophotometer and a Q-switched Nd:YAG laser (Quanta-Ray GCR-130, 532 nm, ∼7 ns fwhm) (*25, 30*). A Ge filter (OCLI, LO2584-9) was placed in front of the sample to block red light of a He−Ne laser from the interferometer. Another Ge filter was placed at the exit of the sample room to protect the MCT detector from the scattering of laser pulses. After two preflashes and subsequent dark adaptation for 1 h, the sample was subjected to four consecutive flashes with 10 s intervals. Single-beam spectra (10 s scan, 20 scans with a scanning mode of double-sided fast return) were recorded twice before the first flash and after individual flashes. The sample was then dark-adapted for 1 h, and this cycle was repeated eight times for one sample. Difference spectra upon individual flashes and a dark-minus-dark spectrum before the first flash were calculated, and the spectra obtained using nine samples were averaged. All spectra were recorded with a resolution of 4 cm^{-1}.

RESULTS

Figure 1 (black lines) shows FTIR spectra in the 1300−1000 cm^{-1} region of moderately hydrated (a) and deuterated (b) films of the PSII core complexes from *T. elongatus*. This frequency region is devoid of strong protein bands arising from the amide I (C═O stretch, ∼1650 cm^{-1}), amide II (CN stretch + NH bend, ∼1550 cm^{-1}), and amide II′ (CN stretch + ND bend, ∼1450 cm^{-1}) vibrations of polypeptide backbones (see Figure S1 of the Supporting Information for the 1800−1100 cm^{-1} region of the spectra). In the deuterated sample, however, the DOD bending vibrations of bulk D_2O show a broad feature around 1210 cm^{-1} (Figure 1b). Indeed, this feature downshifted by ∼10 cm^{-1} when the sample was deuterated using $D_2{}^{18}O$ (Figure 1b, green line). The ^{18}O-induced shift is more clearly seen in a $D_2{}^{16}O$-minus-$D_2{}^{18}O$ double difference spectrum (Figure 1c, red line), which showed a differential signal with peaks at 1225 and 1186 cm^{-1}. In contrast, the spectrum of the hydrated film was unchanged upon $H_2{}^{18}O$ substitution (Figure 1a, green line), which is also shown by a straight line in a double difference spectrum (Figure 1c, blue line). This observation confirms the absence of H_2O-related vibrations in this frequency region. It should be noted that exchangeable protons, especially in the catalytic site of WOC, are basically fully deuterated in this moderately deuterated sample, although protons in hydrophobic domains in the PSII core complexes are hardly replaced with deuterons as shown in its absorption

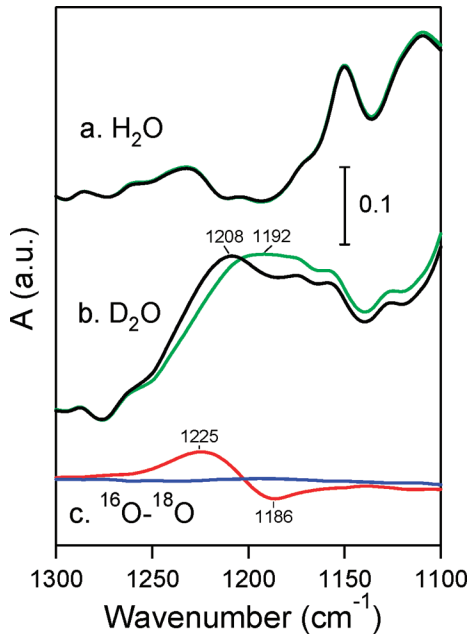

FIGURE 1: FTIR spectra in the 1300−1100 cm^{-1} region of the PSII core complexes from *T. elongatus* moderately hydrated using $H_2{}^{16}O$ (a, black line) and $H_2{}^{18}O$ (a, green line) and deuterated using $D_2{}^{16}O$ (b, black line) and $D_2{}^{18}O$ (b, green line). (c) $H_2{}^{16}O$-minus-$H_2{}^{18}O$ (blue line) and $D_2{}^{16}O$-minus-$D_2{}^{18}O$ (red line) difference spectra of the PSII core complexes.

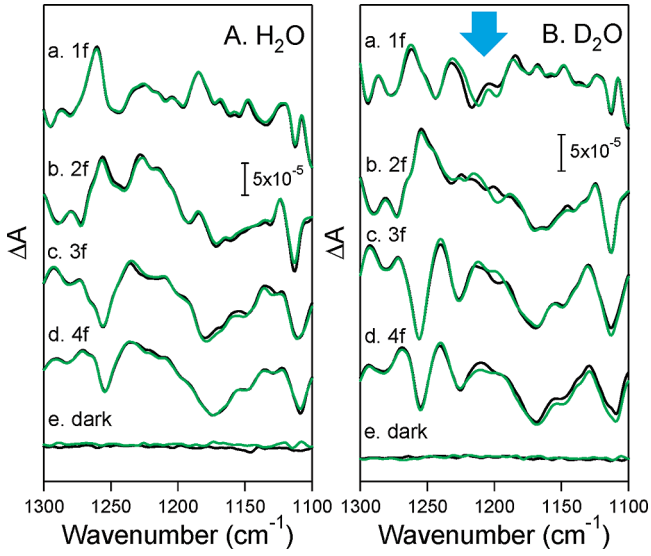

FIGURE 2: Flash-induced FTIR difference spectra in the 1300−1100 cm^{-1} region during the S-state cycle of the WOC in the PSII core complexes moderately hydrated using $H_2{}^{16}O$ (A, black lines) and $H_2{}^{18}O$ (A, green lines) and deuterated using $D_2{}^{16}O$ (B, black lines) and $D_2{}^{18}O$ (B, green lines). Difference spectra were recorded upon the first (a), second (b), third (c), and fourth (d) flash. Dark-minus-dark difference spectra (e) represent noise levels.

spectrum (Figure S1b of the Supporting Information), where the amide II band remains with an intensity comparable to that of the amide II′ band.

Figure 2 shows the flash-induced FTIR difference spectra (1300−1100 cm^{-1}) of the hydrated (A) and deuterated (B) PSII samples during the S-state cycle of the WOC. The spectra at the first (a), second (b), third (c), and fourth (d) flash basically represent the structural changes in the $S_1 \rightarrow S_2$, $S_2 \rightarrow S_3$, $S_3 \rightarrow S_0$, and $S_0 \rightarrow S_1$ transitions (*30*−*32*). The dark-minus-dark spectra (e) represent the noise levels of the difference spectra. The spectra in a wider region (1800−1100 cm^{-1}) involving numerous protein bands (Figures S2 and S3 of the Supporting Information) were virtually identical to the previous ones recorded with similar hydrated (or deuterated) samples (*25, 30*) and showed that the 1300−1100 cm^{-1} region exhibited only relatively weak bands. Among them, the bands at 1260−1255 cm^{-1}, which have positive intensities at the first and second flashes and negative ones at the third and fourth flashes, are the most prominent (Figure 2A,B). These bands have been tentatively assigned to the CO stretches of alcoholic side chains because of the insensitivity to uniform ^{15}N labeling (*33, 34*), although definite assignments have not yet been made. The CN stretching band of a His side chain is found at ∼1112 cm^{-1} (*35, 36*), which is clear at the first flash, but obscured by the Mes bands superimposing this frequency at the second through fourth flashes (Figure 2A,B).

Upon $D_2{}^{18}O$ substitution of the deuterated film, the spectra exhibited small but clear changes around 1200 cm^{-1} (Figure 2Ba−d, green lines; indicated by an arrow). These changes, which were much larger than the noise level (Figure 2Be), were observed in all four flash-induced spectra. In contrast, in the hydrated film, $H_2{}^{18}O$ substitution did not show any appreciable changes in the 1300−1100 cm^{-1} region (Figure 2Aa−d, green lines). It is noted that successful $H_2{}^{18}O$ substitution in the WOC as well as $D_2{}^{18}O$ substitution was confirmed by downshifts of weakly H-bonded OH and OD stretching bands (Figure S4A,B of the Supporting Information), in agreement with the previous results (*25*).

The ^{18}O-induced change was more clearly seen in the $D_2{}^{16}O$-minus-$D_2{}^{18}O$ double difference spectra at individual flashes (Figure 3a−d, red lines). In all of the first through fourth flash spectra, six to eight peaks were observed in the 1250−1150 cm^{-1} region, with intensities larger than the noise level (Figure 3e, red line). This frequency region is in good agreement with that of the DOD bending band of bulk D_2O (Figure 1c, red line). Thus, the observed peaks can be assigned to the DOD bending vibrations of D_2O molecules affected by the S-state transitions. The observation that no meaningful peaks were detected in the $H_2{}^{16}O$-minus-$H_2{}^{18}O$ double difference spectra of the hydrated films (Figure 3a−d, blue lines) supported this assignment. The relatively narrow widths of the DOD bands in Figure 3 (red lines) in comparison with the widths of the bulk D_2O bands (Figure 1c, red line) indicate that the detected D_2O molecules are structurally restricted in proteins or as ligands to the Mn cluster.

Previously, we estimated the miss factors of individual S-state transitions in moderately hydrated films prepared with various relative humidities (*30*). The sample prepared under 95% relative humidity, which was used in this study, exhibited miss factors of 16 ± 1, 19 ± 2, 23 ± 3, and 11 ± 5% for the $S_1 \rightarrow S_2$, $S_2 \rightarrow S_3$, $S_3 \rightarrow S_0$, and $S_0 \rightarrow S_1$ transitions, respectively, based on the average miss factor of 12% estimated for a fully hydrated film. Note that the deuterated film exhibited virtually the same oscillation pattern as the hydrated film (Figure S5 of the Supporting Information). Figure 4 (a−d, red lines) shows corrected $D_2{}^{16}O$-minus-$D_2{}^{18}O$ difference spectra representing pure contributions of individual S-state transitions calculated using the miss factors given above (for the detailed method of calculation, see the Supporting Information), in com-

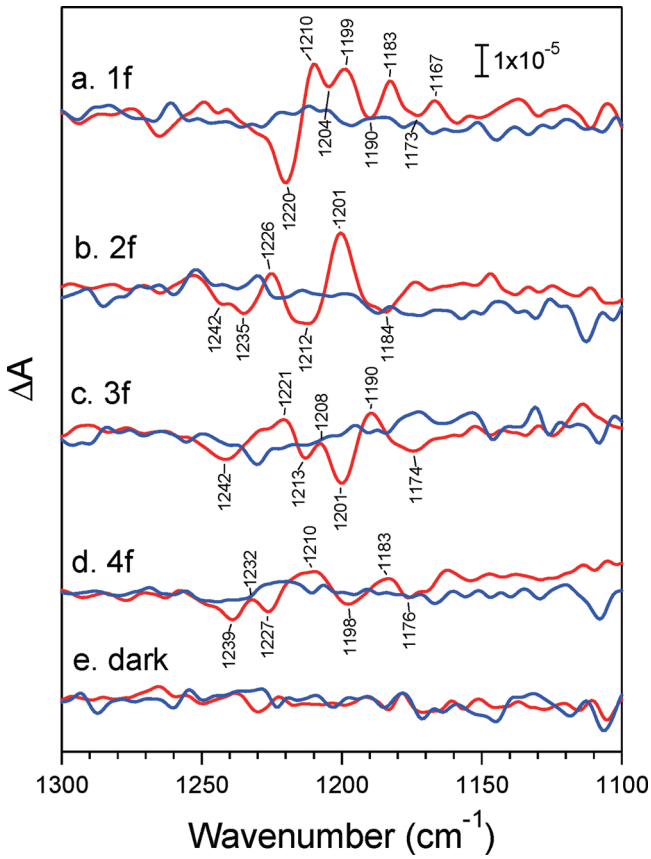

FIGURE 3: $H_2{}^{16}O$-minus-$H_2{}^{18}O$ (blue line) and $D_2{}^{16}O$-minus-$D_2{}^{18}O$ (red line) double difference spectra in the 1300−1100 cm^{-1} region during the S-state cycle of the WOC at the first (a), second (b), third (c), and fourth (d) flashes. Double difference spectra of the dark-minus-dark spectra (e) represent noise levels.

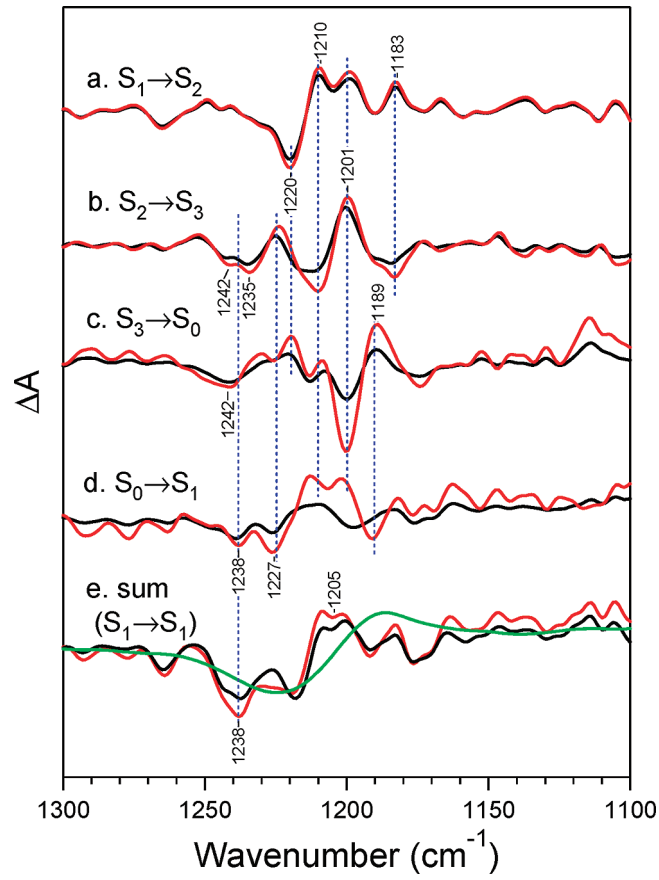

FIGURE 4: Corrected $D_2{}^{16}O$-minus-$D_2{}^{18}O$ double difference spectra representing the pure contribution of the $S_1 \rightarrow S_2$ (a), $S_2 \rightarrow S_3$ (b), $S_3 \rightarrow S_0$ (c), and $S_0 \rightarrow S_1$ (d) transitions (red lines) in comparison with the original spectra at the first through fourth flashes (black lines; identical to the red lines in Figure 3a−d). (e) $D_2{}^{16}O$-minus-$D_2{}^{18}O$ spectra representing completion of one cycle from the S_1 state to the next S_1 state as sums of the corrected spectra for the pure S-state transitions (red line) and of the original spectra at the first through fourth flashes (black line), in comparison with the $D_2{}^{16}O$-minus-$D_2{}^{18}O$ spectrum of bulk D_2O with an inverse sign (green line; deduced from the spectrum in Figure 1c, red line).

parison with the original spectra at the first through fourth flashes (a−d, black line; identical to the red lines in Figure 3a−d). Note that very similar spectra were obtained when the average miss factor of 17% was used for calculation (data not shown). The features of the $S_2 \rightarrow S_3$ (Figure 4b) and $S_3 \rightarrow S_0$ (Figure 4c) spectra were virtually identical to the original second and third flash spectra, respectively, except for the intensity of the $S_3 \rightarrow S_0$ spectrum being much larger than the original one. The $S_0 \rightarrow S_1$ spectrum (Figure 4d) also exhibited a much larger intensity than the original fourth flash spectrum. In addition, the band shapes slightly changed, retaining an overall spectral feature; the peaks slightly shifted and became sharper. The $S_3 \rightarrow S_0$ spectrum exhibited the largest DOD signals among the four spectra as expected from the fact that drastic rearrangement of substrates should take place after O_2 evolution during this transition.

The presence of six to eight peaks in individual $D_2{}^{16}O$-minus-$D_2{}^{18}O$ spectra was unchanged by correction for pure S-state transitions (Figure 4). If one D_2O molecule changes its interaction during the transition, then a maximum of four peaks (two $D^{16}OD$ and two $D^{18}OD$ peaks) should appear in a double difference spectrum. When a deuteron is released from D_2O upon the transition, the bending vibration disappears, and hence, two peaks should be observed. In addition, the overlap of positive and negative peaks may cancel out the intensities to decrease the number of peaks. Thus, the presence of six to eight peaks indicates that at least two D_2O molecules, in a fully deuterated form and not in the form of OD^- or $OD^{\bullet}$, are coupled to the reaction in the WOC in each S-state transition.

Most of the peaks in Figure 4a−d have their counter peaks with opposite signs at different transitions in a manner analogous to that of the protein bands (*30*−*32*), e.g., peaks at 1183 cm^{-1} in the $S_1 \rightarrow S_2$ and $S_2 \rightarrow S_3$ transitions, at ~1201 and ~1210 cm^{-1} observed in all four transitions, at 1220 cm^{-1} in the $S_1 \rightarrow S_2$ and $S_3 \rightarrow S_0$ transitions, and at ~1227 cm^{-1} in the $S_2 \rightarrow S_3$ and $S_0 \rightarrow S_1$ transitions. These peaks probably represent a series of reactions or interaction changes of D_2O molecules at the catalytic site during the S-state cycle.

In contrast, counter peaks were not readily found for some peaks, e.g., relatively broad negative peaks at ~1240 cm^{-1} in the $S_2 \rightarrow S_3$ and $S_3 \rightarrow S_0$ transitions. This is reasonable because two water molecules have to be consumed during the S-state cycle, and hence, all the water bands do not oscillate. In fact, the spectrum as a sum of the four corrected spectra of the S-state transitions, representing the difference upon completion of one cycle from the initial S_1 state to the next S_1 state, did not cancel out the bands but exhibited relatively strong negative and positive features at ~1238 and ~1205 cm^{-1}, respectively

(Figure 4e, red line). Note that a corresponding spectrum obtained using the original flash-induced spectra, which would represent the S_1-minus-S_1 difference spectrum under the assumption that the miss factors all equal zero, also exhibited a similar feature (Figure 4e, black line). A negative band on the higher-frequency side in the $D_2{}^{16}O$-minus-$D_2{}^{18}O$ spectrum upon completion of one cycle implies consumption of water molecules.

If substrate is taken up from bulk water, the DOD bands upon one cycle (Figure 4e, red line) should agree with those of bulk D_2O. However, both of the negative and positive bands were observed at frequencies slightly higher than those of the bulk D_2O bands (Figure 4e, green line). It is known that the frequencies of HOH or DOD bending vibrations shift upward upon hydrogen bond formation and water clusters exhibit bending frequencies even higher than those of liquid water (*27, 28*), whereas an interaction with a metal ion shifts the frequency downward (*37*). Thus, the observed DOD frequencies which are higher than those of bulk D_2O may suggest that substrate is inserted into the WOC from a water cluster present in the water pathway in the protein between the WOC and the lumenal side. In solutions, the rate of access of bulk water to the catalytic site of the WOC should be faster than the millisecond time scale, which is the measurable exchange rate of substrate in a fast phase (*10, 11*). Thus, detection of internal water could indicate a rather slow access of bulk water (on a time scale of seconds) to the inside of the protein at least in the moderately hydrated (deuterated) PSII samples used in this study. The substrate insertion may occur in the $S_2 \rightarrow S_3$, $S_3 \rightarrow S_0$, and possibly $S_0 \rightarrow S_1$ transitions, which exhibited negative bands at ~1240 cm^{-1} that can be attributed to substrate.

Similar analysis in the OD stretching region of the flash-induced difference spectra of the sample deuterated with $D_2{}^{16}O$ (Figure 5) supported this view. The difference spectrum upon completion of one cycle (Figure 5e, red line), which was calculated as a sum of the four corrected spectra of pure S-state transitions (Figure 5a−d, red lines), exhibited a clear negative band at ~2694 cm^{-1} in the weakly D-bonded OD stretching region. This band is significantly different from the OD band of bulk D_2O with a broad feature at a lower frequency (Figure 5, green line) and, hence, probably arises from internal water molecules having weakly D-bonded OD bonds. The negative intensity originates from the negative band at 2695 cm^{-1} at the $S_2 \rightarrow S_3$ transition and a negative shoulder at a similar position in the $S_3 \rightarrow S_0$ transition, suggesting the insertion of substrate in these transitions. The major negative band at 2678 cm^{-1} in the $S_3 \rightarrow S_0$ transition seems to correspond to the positive band at 2681 cm^{-1} in the $S_1 \rightarrow S_2$ transition, indicating the reaction (a proton release or the change from a weak H-bond to a strong one) of the water molecule already bound to the Mn cluster.

The insertion of substrate in the $S_2 \rightarrow S_3$ and $S_3 \rightarrow S_0$ transitions is also consistent with our previous FTIR data which showed that these transitions are more sensitive to dehydration than other transitions (*23, 30*). Because mass spectrometry studies showed that two substrate molecules are already bound to the WOC in the S_2 state (*2, 11*), the water molecule inserted in the $S_2 \rightarrow S_3$ transition could be used as a substrate in the next cycle.

The results of this FTIR study show that at least two water molecules, not in any deprotonated forms, are coupled to the reactions at the catalytic site of the WOC during each S-state transition. Two substrate water molecules should be involved in these water molecules. However, because release of a proton from substrate takes place probably in the $S_0 \rightarrow S_1$, $S_2 \rightarrow S_3$, and $S_3 \rightarrow S_0$ transitions (*38*), the number of DOD bands cannot be explained by only substrate water. This indicates that some water molecules other than substrate exist in the vicinity of the Mn cluster and are involved in the reaction. Probably, they function as ligands to the Mn and Ca ions or form a hydrogen bond network around the Mn cluster to participate in the reaction mechanism of water oxidation. This view is consistent with the previous ESEEM and ENDOR results, which showed the presence of several exchangeable protons in the vicinity of the Mn cluster in the S_0, S_1, and S_2 states (*12−15*). Also, this is consistent with the recent structural models of the WOC and the mechanism of water oxidation proposed by quantum chemical calculations (*39−41*) based on the X-ray crystal structures and the EXAFS data (*5−7*).

In this study, we have for the first time detected the DOD vibrations of D_2O molecules coupled to the S-state transitions in the WOC. To the best of our knowledge, this is the first report of detection of the bending vibrations of functional water molecules in active sites of proteins. Monitoring the

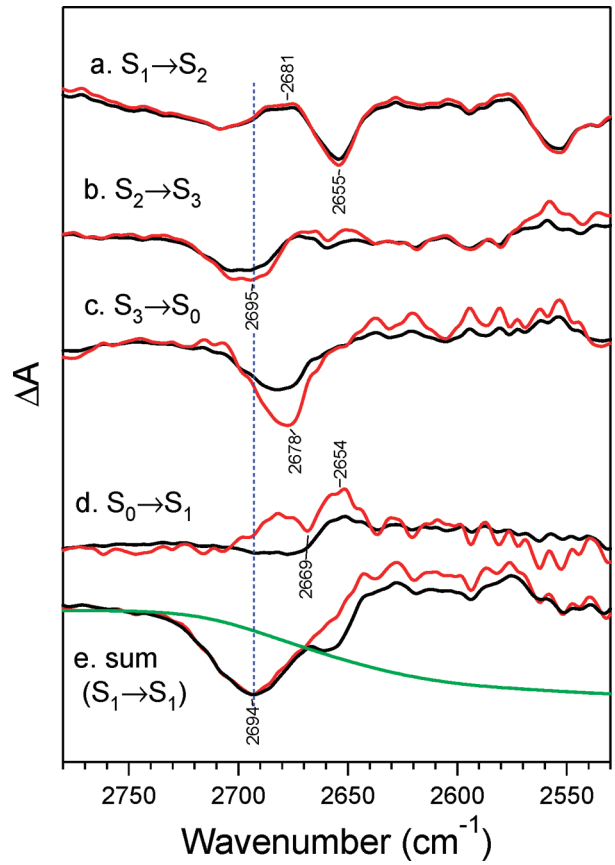

FIGURE 5: Corrected FTIR difference spectra in the OD stretching region representing the pure contribution of the $S_1 \rightarrow S_2$ (a), $S_2 \rightarrow S_3$ (b), $S_3 \rightarrow S_0$ (c), and $S_0 \rightarrow S_1$ (d) transitions (red lines) in comparison with the original spectra at the first through fourth flashes for the sample deuterated with $D_2{}^{16}O$ (black lines). (e) Difference spectra representing completion of one cycle from the S_1 state to the next S_1 state as sums of the corrected spectra for the pure S-state transitions (red line) and of the original spectra at the first through fourth flashes (black line), in comparison with the spectrum of bulk D_2O with an inverse sign (green line).

water reactions using the DOD bending bands, together with OH(D) stretching bands, and careful spectral analysis in combination with chemical perturbation (e.g., addition of substrate analogues and metal substitution) and mutagenesis studies will provide crucial information that will clarify the molecular mechanism of the photosynthetic water oxidation as well as other enzymatic reactions involving functional water molecules.

SUPPORTING INFORMATION AVAILABLE

FTIR spectra in the 1800−1100 cm^{-1} region of moderately hydrated and deuterated PSII core complexes, their flash-induced FTIR difference spectra in the same region and in the OH (3720−3500 cm^{-1}) and OD (2770−2550 cm^{-1}) stretching regions, the oscillation patterns of the FTIR signal of the WOC in the hydrated and deuterated samples, and the method for calculation of the corrected spectra representing pure S-state transitions. This material is available free of charge via the Internet at http://pubs.acs.org.

REFERENCES

1. Debus, R. J. (1992) The manganese and calcium ions of photosynthetic oxygen evolution. *Biochim. Biophys. Acta 1102*, 269–352.
2. Hillier, W., and Messinger, J. (2005) Mechanism of photosynthetic oxygen production. In *Photosystem II: The Light-Driven Water: Plastoquinone Oxidoreductase* (Wydrzynski, T., and Satoh, K. Eds.) pp 567−608, Springer, Dordrecht, The Netherlands.
3. McEvoy, J. P., and Brudvig, G. W. (2006) Water-splitting chemistry of photosystem II. *Chem. Rev. 106*, 4455–4483.
4. Renger, G. (2007) Oxidative photosynthetic water splitting: Energetics, kinetics and mechanism. *Photosynth. Res. 92*, 407–425.
5. Ferreira, K. N., Iverson, T. M., Maghlaoui, K., Barber, J., and Iwata, S. (2004) Architecture of the photosynthetic oxygen-evolving center. *Science 19*, 1831–1838.
6. Loll, B., Kern, J., Saenger, W., Zouni, A., and Biesiadka, J. (2005) Towards complete cofactor arrangement in the 3.0 Å resolution structure of photosystem II. *Nature 438*, 1040–1044.
7. Yano, J., Kern, J., Sauer, K., Latimer, M. J., Pushkar, Y., Biesiadka, J., Loll, B., Saenger, W., Messinger, J., Zouni, A., and Yachandra, V. K. (2006) Where water is oxidized to dioxygen: Structure of the photosynthetic Mn_4Ca cluster. *Science 314*, 821–825.
8. Yano, J., Kern, J., Irrgang, K. D., Latimer, M. J., Bergmann, U., Glatzel, P., Pushkar, Y., Biesiadka, J., Loll, B., Sauer, K., Messinger, J., Zouni, A., and Yachandra, V. K. (2005) X-ray damage to the Mn_4Ca complex in single crystals of photosystem II: A case study for metalloprotein crystallography. *Proc. Natl. Acad. Sci. U.S.A. 102*, 12047–12052.
9. Grabolle, M., Haumann, M., Muller, C., Liebisch, P., and Dau, H. (2006) Rapid loss of structural motifs in the manganese complex of oxygenic photosynthesis by X-ray irradiation at 10−300 K. *J. Biol. Chem. 281*, 4580–4588.
10. Hillier, W., and Wydrzynski, T. (2001) Oxygen ligand exchange at metal sites: Implications for the O_2 evolving mechanism of photosystem II. *Biochim. Biophys. Acta 1503*, 197–209.
11. Hillier, W., and Wydrzynski, T. (2004) Substrate water interactions within the Photosystem II oxygen evolving complex. *Phys. Chem. Chem. Phys. 6*, 4882–4889.
12. Kawamori, A., Inui, T., Ono, T., and Inoue, Y. (1989) ENDOR study on the position of hydrogens close to the manganese cluster in S_2 state of photosystem II. *FEBS Lett. 254*, 219–224.
13. Fiege, R., Zweygart, W., Bittl, R., Adir, N., Renger, G., and Lubitz, W. (1996) EPR and ENDOR studies of the water oxidizing complex of Photosystem II. *Photosynth. Res. 48*, 227–237.
14. Aznar, C. P., and Britt, R. D. (2002) Simulations of the ^1H electron spin echo-electron nuclear double resonance and ^2H electron spin echo envelope modulation spectra of exchangeable hydrogen nuclei coupled to the S_2-state photosystem II manganese cluster. *Philos. Trans. R. Soc. London, Ser. B 357*, 1359–1365.
15. Britt, R. D., Campbell, K. A., Peloquin, J. M., Gilchrist, M. L., Aznar, C. P., Dicus, M. M., Robblee, J., and Messinger, J. (2004) Recent pulsed EPR studies of the Photosystem II oxygen-evolving complex: Implications as to water oxidation mechanisms. *Biochim. Biophys. Acta 1655*, 158–171.
16. Yamada, H., Mino, H., and Itoh, S. (2007) Protons bound to the Mn cluster in photosystem II oxygen evolving complex detected by proton matrix ENDOR. *Biochim. Biophys. Acta 1767*, 197–203.
17. Su, J. H., Lubitz, W., and Messinger, J. (2008) Probing mode and site of substrate water binding to the oxygen-evolving complex in the S_2 state of photosystem II by ^{17}O-HYSCORE spectroscopy. *J. Am. Chem. Soc. 130*, 786–787.
18. Chu, H.-A., Hillier, W., Law, N. A., and Babcock, G. T. (2001) Vibrational spectroscopy of the oxygen-evolving complex and of manganese model compounds. *Biochim. Biophys. Acta 1503*, 69–82.
19. Noguchi, T., and Berthomieu, C. (2005) Molecular analysis by vibrational spectroscopy. In *Photosystem II: The Light-Driven Water:Plastoquinone Oxidoreductase* (Wydrzynski, T., and Satoh, K. Eds.) pp 367−387, Springer, Dordrecht, The Netherlands.
20. Noguchi, T. (2007) Light-induced FTIR difference spectroscopy as a powerful tool toward understanding the molecular mechanism of photosynthetic oxygen evolution. *Photosynth. Res. 91*, 59–69.
21. Noguchi, T. (2008) Fourier transform infrared analysis of the photosynthetic oxygen-evolving center. *Coord. Chem. Rev. 252*, 336–346.
22. Debus, R. J. (2008) Protein ligation of the photosynthetic oxygen-evolving center. *Coord. Chem. Rev. 252*, 244–258.
23. Noguchi, T. (2008) FTIR detection of water reactions in the oxygen-evolving center of photosystem II. *Philos. Trans. R. Soc. London, Ser. B 363*, 1189–1195.
24. Noguchi, T., and Sugiura, M. (2000) Structure of an active water molecule in the water-oxidizing complex of photosystem II as studied by FTIR spectroscopy. *Biochemistry 39*, 10943–10949.
25. Noguchi, T., and Sugiura, M. (2002) FTIR detection of water reactions during the flash-induced S-state cycle of the photosynthetic water-oxidizing complex. *Biochemistry 41*, 15706–15712.
26. Venyaminov, S. Y., and Prendergast, F. G. (1997) Water (H_2O and D_2O) molar absorptivity in the 1000−4000 cm^{-1} range and quantitative infrared spectroscopy of aqueous solutions. *Anal. Biochem. 248*, 234–245.
27. Xantheas, S. S., and Dunning, T. H., Jr. (1993) *Ab initio* studies of cyclic water clusters $(H_2O)_n$, $n = 1-6$. I. Optimal structures and vibrational spectra. *J. Chem. Phys. 99*, 8774–8792.
28. Sadlej, J. (2002) *Ab initio* study of bending modes in water cage clusters, $(H_2O)_n$, $n = 6-10$. *Int. J. Quantum Chem. 90*, 1191–1205.
29. Sugiura, M., and Inoue, Y. (1999) Highly purified thermo-stable oxygen-evolving photosystem II core complex from the thermophilic cyanobacterium *Synechococcus elongatus* having His-tagged CP43. *Plant Cell Physiol. 40*, 1219–1231.
30. Noguchi, T., and Sugiura, M. (2002) Flash-induced FTIR difference spectra of the water oxidizing complex in moderately hydrated photosystem II core films: Effect of hydration extent on S-state transitions. *Biochemistry 41*, 2322–2330.
31. Noguchi, T., and Sugiura, M. (2001) Flash-induced Fourier transform infrared detection of the structural changes during the S-state cycle of the oxygen-evolving complex in photosystem II. *Biochemistry 40*, 1497–1502.
32. Hillier, W., and Babcock, G. T. (2001) S-state dependent Fourier transform infrared difference spectra for the photosystem II oxygen evolving complex. *Biochemistry 40*, 1503–1509.
33. Noguchi, T., and Sugiura, M. (2003) Analysis of flash-induced FTIR difference spectra of the S-state cycle in the photosynthetic water-oxidizing complex by uniform ^{15}N and ^{13}C isotope labeling. *Biochemistry 42*, 6035–6042.
34. Kimura, Y., Mizusawa, N., Ishii, A., Yamanari, T., and Ono, T. (2003) Changes of low-frequency vibrational modes induced by universal ^{15}N- and ^{13}C-isotope labeling in S_2/S_1 FTIR difference spectrum of oxygen-evolving complex. *Biochemistry 42*, 13170–13177.
35. Noguchi, T., Inoue, Y., and Tang, X.-S. (1999) Structure of a histidine ligand in the photosynthetic oxygen-evolving complex as studied by light-induced Fourier transform infrared difference spectroscopy. *Biochemistry 38*, 10187–10195.
36. Kimura, Y., Mizusawa, N., Ishii, A., and Ono, T. (2005) FTIR detection of structural changes in a histidine ligand during S-state cycling of photosynthetic oxygen-evolving complex. *Biochemistry 44*, 16072–16078.

37. Manceron, L., Loutellier, A., and Perchard, J. P. (1985) IR spectroscopy and photosensitivity of the H_2O-Li complex trapped in a krypton matrix. *Chem. Phys. 92*, 75–89.
38. Schlodder, E., and Witt, H. T. (1999) Stoichiometry of proton release from the catalytic center in photosynthetic water oxidation: Reexamination by a glass electrode study at pH 5.5−7.2. *J. Biol. Chem. 274*, 30387–30392.
39. Siegbahn, P. E. M., and Lundberg, M. (2005) The mechanism for dioxygen formation in PSII studied by quantum chemical methods. *Photochem. Photobiol. Sci. 4*, 1035–1043.
40. Zein, S., Kulik, L. V., Yano, J., Kern, J., Pushkar, Y., Zouni, A., Yachandra, V. K., Lubitz, W., Neese, F., and Messinger, J. (2008) Focusing the view on nature's water-splitting catalyst. *Philos. Trans. R. Soc. London, Ser. B 363*, 1167–1177.
41. Sproviero, E. M., Gascon, J. A., McEvoy, J. P., Brudvig, G. W., and Batista, V. S. (2008) Quantum mechanics/molecular mechanics study of the catalytic cycle of water splitting in photosystem II. *J. Am. Chem. Soc. 130*, 3428–3442.

BI801580E